Journal of Visualization, Vol. 11, No. 3 (2008)213-220

**Regular Paper**

# Dilatation and Pattern Formation of Cells in Internally Heated Convection

Tasaka, Y.*[1], Yonekura, K.*[1, 2], Takeda, Y.*[1] and Yanagisawa, T.*[3]

*1 Division of Energy and Environment Systems, Graduate School of Engineering, Hokkaido University, N13W8, Sapporo, 060-8628, Japan. E-mail: tasaka@eng.hokudai.ac.jp
*2 Nissan Motor Co., Ltd., 6-1 Tsurumi-ku, Yokohama, 230-0053, Japan.
*3 Institute for Research on Earth Evolution, Japan Agency for Marine-Earth Science and Technology, 2-15 Natsushima, Yokosuka, 237-0061, Japan.

Received 20 September 2007
Revised 26 March 2008

***Abstract*** : The dilatation and the pattern formation of convection cells in natural convection driven by internal heat generation, first investigated during the 1970s, are reexamined in this paper using an improved experimental apparatus in order to reduce uncertainties as much as possible. The convective motion in the fluid layer was visualized using reflecting particles (Kalliroscope). Cell dilatation was confirmed in the improved experimental apparatus and then investigated quantitatively by extracting the pattern wavenumber from Fourier analysis of the images recorded by a digital camera. The pattern wavenumber was found to decrease with increasing Rayleigh number. We compare our results with earlier investigations and discuss the influence of the thermal boundary condition at the bottom of the fluid layer on the variation of the wavenumber. Two different structures were observed in the same fluid layer at a relatively high Rayleigh number; an additional cell appears in the original cell (Double cell structure) and the descending flow region around the center of the cell expands laterally like a spoke of wheels (Spoke-like structure). Factors for the formation of such complex structures are discussed.

***Keywords*** : Visualization, Natural Convection, Pattern Formation, Anisotropic Flakes.

## 1. Introduction

Natural convection induced by internal heat generation exists everywhere in nature. Examples are motions in the atmosphere (e.g., Tritton, 1975) where heat is generated by absorption of sunlight, and mantle convection in the earth (e.g., Turcotte et al., 2001) where heat is generated by radioactive decay of isotopes. The effects of internal heat generation, however, have received little attention even though it is of equal or even greater importance (at least in so far as its effect on the flow pattern (e.g., Schubert et al., 2001)) than, say, a temperature dependent viscosity.

Studies of internally heated convection in a shallow fluid layer reported a transition process of the convection cells: Hexagonal cells are formed at a relatively small Rayleigh number and then expand as the Rayleigh number increases (Tritton and Zarraga, 1967). A descending flow region around the center of the cell spreads to the lateral of the cell like a spoke of wheels at a higher Rayleigh number (Ichikawa et al., 2006). The cell structure collapses and descending flow sheet becomes dominant at a further high Rayleigh number (Carrigan, 1985). The cell dilatation is typical in comparison with standard Rayleigh-Bénard convection, but theoretical studies e.g., by Roberts (1967) could not clarify the origin of this phenomenon. Furthermore, Schwiderski and Schwab (1971) concluded that cell dilatation is not an intrinsic feature of the problem, but instead is induced by non-uniformity of internal heat generation in the experimental apparatus. To our knowledge there have been no further experimental investigations of cell dilatation until now. In this paper we reinvestigate the problem of cell dilatation and study it in greater detail than previous method allowed.

Two criticisms of past studies that we address in this work are: (1) horizontal variation of the amount of internal heat generation induced by non-uniformity of electric conductivity of the fluid, (2) non-adiabatic boundary condition at the bottom of the fluid layer. In our experiments we used a more precise experimental setup and minimized or eliminated the difficulties described above. We also studied the variation of the cell dilatation with Rayleigh number more systematically by measuring the pattern wavenumber using the Fourier transform of images of the convective motion taken by a digital camera. Transition of the cell structure subsequent to the cell dilatation was also observed.

## 2. Experimental Setup

A horizontal fluid layer with thickness $L$ generates heat uniformly at rate $H$ per unit time and per unit volume. To focus our study on the influence of internal heat generation, we set the thermal boundary conditions on the top and the bottom plate as isothermal and adiabatic, respectively. The control parameter in this problem is the internal Rayleigh number, defined as

$$R_{\mathrm{I}} = \frac{g\beta HL^5}{2\lambda\kappa\upsilon},$$

where $g$ is gravity, $\beta$, $\lambda$, $\kappa$ and $\nu$ are thermal expansion coefficient, thermal conductivity, thermal diffusivity and kinematic viscosity of the fluid respectively. Instead of $R_{\mathrm{I}}$, we use the reduced internal Rayleigh number $R_{\mathrm{I}}^* = R_{\mathrm{I}} / R_{\mathrm{c}}$, where $R_{\mathrm{c}}$ is critical Rayleigh number; Roberts's calculations yield $R_{\mathrm{c}} = 1386$, estimated theoretically (Roberts, 1967).

Our experimental apparatus was designed and constructed to minimize non-uniformities in the internal heat generation and to make the adiabatic boundary condition at the bottom of the fluid layer. Figure 1 shows a schematic illustration of the apparatus. The apparatus mainly consists of two parts, a fluid container and a cooling part as the lid of the container. All but the bottom plate of the fluid container is made of Plexiglas with a thickness of 10 mm. The horizontal area of the container is a square of sides 210 mm, the plate separation is 7 mm, yielding an aspect ratio of 30. In order to make the adiabatic condition, 6 mm vacuumed glass with 0.2 mm vacuumed space (to $10^{-6}$ atm), is used as the bottom plate. The heat flux through the bottom plate, which is estimated from heat conduction in the low-pressure air and approximated blackbody radiation, is reduced to one third of the maximum heat flux of a Plexiglas plate, which was used in Schwiderski and Schwab (1971).

The lid of the container, the cooling part, is an aluminum block 18 mm thick. The temperature at the bottom surface of this block was kept constant by flowing water over the lid. The temperature of the flowing water was controlled by a thermostatic bath to within ± 0.1 °C. Biot number, which indicates an evaluation of the thermal boundary condition, is roughly estimated as $Bi = (L_{\mathrm{p}}/\lambda_{\mathrm{p}})/(L/\lambda) = 0.007$ in our experiment, where $L_{\mathrm{p}}$ and $\lambda_{\mathrm{p}}$ are respectively the thickness of the top plate and thermal conductivity of aluminum. This value is enough small for regarding the thermal boundary condition as isothermal. The water temperature was initially set to room temperature to avoid an initial perturbation in the fluid and heat flux through the lateral wall of the container. The bottom of the aluminum block was coated with black paint for the sake of electric insulation and visualization. The height of the fluid layer (7 mm) was about 1.5 times greater than that used in previous studies (Tritton and Zarraga, 1967; Schwiderski and Schwab, 1971). Therefore, to achieve the same internal Rayleigh number as used in previous experiments, the amount of internal heat generation was reduced to one eighth of that used in previous studies. Typical temperature difference in the fluid layer is estimated to be about 2 °C at the minimum by solving the heat conduction equation.

A 0.5 wt % potassium chloride (KCl) solution was used as the ionic fluid. In comparison with past studies, this ionic fluid has a small electric conductivity; furthermore, it is only weakly dependent on temperature. A stabilized AC power supply, NF model EPX4104, was used for electric heating to avoid bubble generation at the electrodes. Since the electric conductivity of an ionic fluid depends on temperature, the electric current passing through the fluid layer slightly increases with temperature. In our experiments the current increased by about 8 % of its initial value. This ratio of increase of electric current is smaller than that in Schwiderski and Schwab (1971) by two third at the same range of $R_I$ with our experiment. This equilibrium value was used in calculating the internal Rayleigh number $R_I$, namely, uniform internal heat generation is assumed. The heat per unit time and per unit volume $H$ was derived as $H = EI/V$, where $E$ and $I$ are effective values of electric current and voltage, $V$ is the volume of the fluid layer. Typical values of them for $R_I^* = 6$ are; $E = 48.5$ V, $I = 326.54$ mA and then $H = 48970.9$ W/m$^3$.

We used reflecting particles (Kalliroscope flakes, AQ-1000 rheoscopic concentration, Thoroddsen et al., (1999); Tasaka et al., (2007)) to visualize the fluid motion. It is a suspension of microscopic crystalline platelets (the main ingredient of the platelet is guanine, which has 1.62 g/cm$^3$ in density, and the size of the platelet is $60 \times 30 \times 0.07$ μm), these platelets are arranged parallel to the planes of shear flow. A thin horizontal slice of the fluid layer was illuminated with a light sheet at mid-depth, and photographs were taken looking up through the bottom of the fluid container by a Nikon D1X digital camera. Each photograph had about $1000 \times 1000$ pixels.

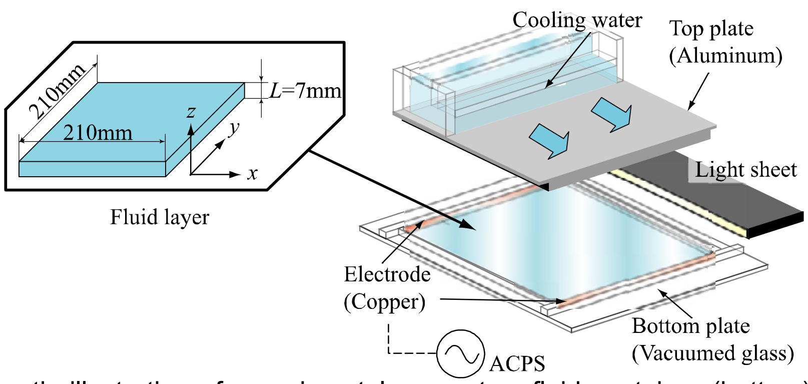


Fig. 1. Schematic illustration of experimental apparatus; fluid container (bottom), cooling part (top) and fluid layer (left). Electric current passes through the fluid layer parallel to the $x$ -direction.

# 3. Results and Discussions

## 3.1 Polygonal Shape of the Cell

Photographs of the convection patterns for three values of $R_I^*$ are shown in Fig. 2. Each picture was taken after that convection pattern relaxed to a time-independent steady state. This took about 2 hours in our experiments. The white square in the upper right corner of these photographs is an indication of $2L$. A light sheet was emitted from above in these photographs. The copper electrodes were located on both sides; then the direction of the electric current in these photographs is the horizontal direction, i.e., the $x$-direction.

There are cells with irregular shape in every photograph taken at different $R_I^*$ and this is in accord with the results of past studies (Tritton and Zarraga, 1967; Schwiderski and Schwab, 1971). As it is well known, the shape of a convection cell in Rayleigh-Bénard convection at Rayleigh numbers slightly larger than the critical Rayleigh number is a two-dimensional roll. In these experiments, however, the convection cell has a polygonal (nearly hexagonal) shape and is three-dimensional. Moreover, the fluid descends from the center of a cell and ascends along the polygonal outer boundary (see Fig. 6(a); such flow direction cannot be distinguished in the photographs). The descending flow at the center is dominant in the internally heated convection because the convective motion is induced by the separation of thermal boundary layer from the top boundary. Thicker fluid layer or rapid heating of the fluid layer sometime induce irregularity of the cells in Rayleigh-Bénard convection because of imperfection of linearity of the initial temperature profile. We performed the same experiment with a thinner fluid layer with 3 mm thickness and the patterns were similar. The convection induced by internal heat generation probably has a wider permissible range for wavenumber of the disturbance. Schwiderski and Schwab (1971) pointed out that the arrangement of cells depends on the direction of the electric current. However, in our experiments we could find no significant dependence of the arrangement on the direction of the current.

Because we used a thicker fluid layer in order to reduce internal heat generation non-uniformity, we expected the cell dilatation to be much weaker in our experiments compared to previous studies (Tritton and Zarraga, 1967; Schwiderski and Schwab, 1971). However, as the photographs illustrate, the convection cells clearly expand while keeping their shape as $R_I$* increases.

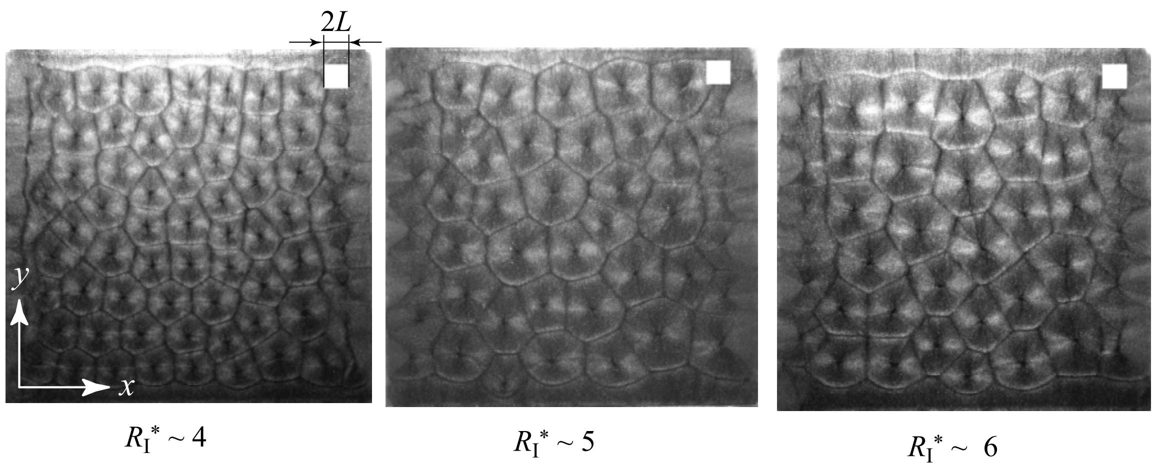


Fig. 2. Dilatation of convection cell shown in visualized pictures, where white squares on photographs are indication of $2L$.

### 3.2 Dilatation of the Cell

In internally heated convection, a convection cell expands with increasing $R_I$* as shown in Fig. 2. These results are qualitatively similar to the earlier studies (Tritton and Zarraga, 1967; Schwiderski and Schwab, 1971). For a quantitative comparison with earlier studies, we have studied the cell dilatation by extracting the pattern wavenumber from the Fourier transform of our high-resolution digital images.

Each element in a visualized image of convective motion has brightness information with 256 levels, and this brightness is modulated in space by the convective motion of a cell. Therefore, we can determine the cell wavenumber from a Fourier analysis of this brightness variation. The brightness depends on the arrangement of the Kalliroscope flakes; it becomes the minimum at the boundary between the cells and the center of the cells where the vertical flow is dominant in this configuration. Details of the wavenumber analysis are explained as follows by using an example shown in Fig. 3. Figure 3(a) is an analyzed image expressed by elements of about 1050 times 1050 pixels, where physical size of the image is about 210 mm times 210 mm; then spatial resolution is approximately 0.2 mm/pixel. Brightness variation extracted from the image along a horizontal line expressed as a white line drawn in Fig. 3(a) has several periods according to the number of cells in the image (Fig. 3(b)). All of available brightness variations are analyzed by discrete Fourier transform with Hanning window function. Figure 3(c) is an average spectrum obtained as above, showing a peak near $n = 20$, where $n$ represents the number of waves in a brightness variation. This result is consistent with the number of cells lined on the horizontal or the vertical direction. The value of $n$ of the peak, $< n >$, is determined by a parabolic approximation of neighboring points around the maximum point in an averaged spectrum as shown in Fig. 3(c). The half-width of this parabola expresses its error, which contains various uncertainties caused by effects of the side boundary, irregularity on the form of the convection cells, etc. The reciprocal of $< n >$ corresponds to the mean length of lines passing through a circle which has the same area that a regular hexagonal cell was. One cell contains two periods of the brightness variation. According to this relation, $< n >$ can be converted to mean wavenumber of cells $k$.

The analysis with Fourier transform was carried out to determine a wavenumber for parallel ($x$-direction), $k_x$, and perpendicular ($y$-direction) to the direction of the electric current, $k_y$. However, there is no typical difference on the wavenumber between the directions.

Figure 4 shows the variation of the wavenumber $k$ estimated by image processing; the error bars for $R_I$* are determined from the deviation of the measured electric current and voltage in the AC power supply. The results of Schwiderski and Schwab (1971) and the critical wavenumber determined theoretically by Roberts (1967) are also shown. Solid symbols represent the wavenumber determined from the temperature field in the same apparatus (Tasaka et al., 2005). The wavenumber decreases monotonically with respect to $R_I$*. The solid line shows an approximate linear function of present data; the slope is around -0.23. The wavenumber decreases linearly with respect to $R_I$* until $R_I$* = 8 and saturates beyond this value. This saturation might be induced by the influence of the lateral boundary. The present results are slightly smaller than the other results for each $R_I$*, but the slope of the variation is similar. This difference might be caused by; (i) differences in the problematic thermal boundary condition - we used an adiabatic boundary condition, while Schwiderski and Schwab (1971) used Plexiglas, which has no negligible thermal conductivity, (ii) differences in the mean temperature of the system – physical properties, e.g., electric conductivity and kinematic viscosity, slightly depend on the temperature. The cell dilatation may be related to the enhancement of “cold plume”; the cold plume, which is a separated thermal boundary layer from the top boundary, induces convective motion by sweeping high temperature fluid at the lower part of the fluid layer. This sweep is enhanced with increasing Rayleigh number.

### *3.3 Double Cell and Spoke-Like Structures*

The expanded cell evolves from the hexagonal structure to more complex structure at further high Rayleigh numbers. Figure 5 shows the visualized photographs of the cell shapes observed at $R_I^* \sim 20$. The hexagonal cell evolves into a more irregular shape by the effect of container size and any other intrinsic factors. An additional cell is formed inside the original cell shown in Fig. 5(a) and thus it has a double structure (see Fig. 6(b)). This is the double cell structure reported in Schwiderski and Schwab (1971). They mentioned that the double cell structure is transitional and collapses into small-polygonal cells. In our observation, however, the structure was maintained for 2 hours without collapse. There is maybe a limit for which the double cell structure stably exists. In Fig. 5(b) the descending flow region around the center of the cell expands laterally like a spoke of wheels (see Fig. 6(c)). This is similar to the spoke-like structure predicted by a numerical simulation in Ichikawa, et

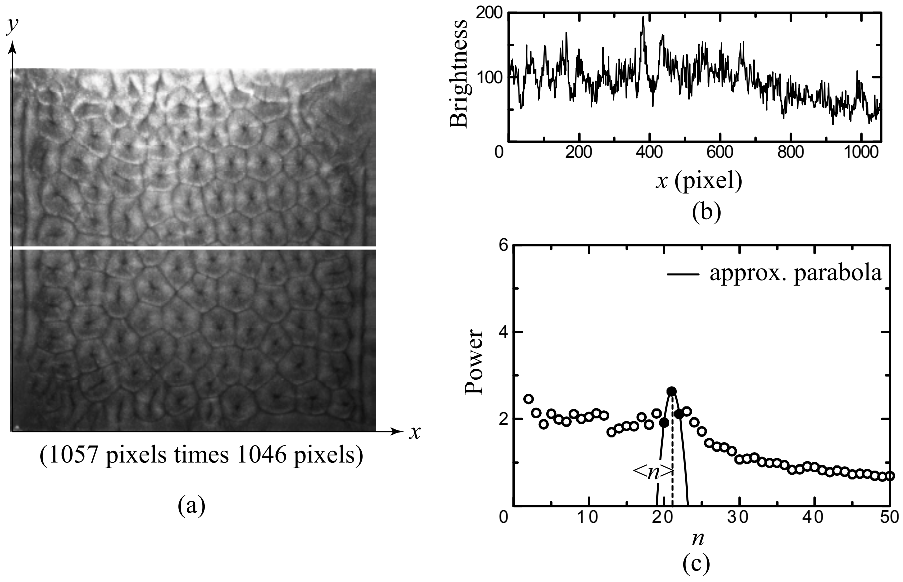


Fig. 3. Periodic fluctuation of brightness variation extracted from a visualized picture; (a) Visualized photograph of a fluid layer, (b) Brightness information extracted from the photograph along a horizontal white line drawn in the photograph, (c) Averaged spectrum of brightness information over space the fluid layer, where $n$ represents the number of waves in the brightness variation for 210 mm.

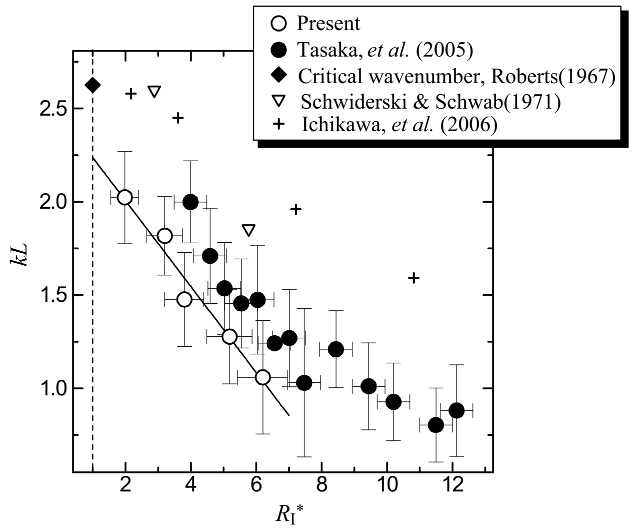


Fig. 4. Variation of wavenumber $k$ with respect to $R_I$*, where the solid line expresses an approximated linear function of this works determined from visualized images.

al. (2006). These structures were observed together in the present study. It has not been clarified what are the factors that take place on the transition from the regular hexagon to such more complex structures. However, hypotheses are conducted from measurements of the temperature distribution in the cell (Tasaka et al., 2005) and observation of the structures: Ascending flow region at the outline of the cell is distinguished around apexes of the hexagonal cell with increasing Rayleigh number, and it obstructs the uniform expansion of the descending flow region laterally (Tasaka et al., 2005). The spoke-like structure may be formed as the result of this non-uniform expansion of the descending flow region. The double cell structure has never been observed in ideal systems of the numerical simulation and is usually observed in relatively irregular hexagons in the experiment as shown in Fig. 5(a). The structure may be formed when the asymmetry of the descending flow region in the expanded cell becomes large.

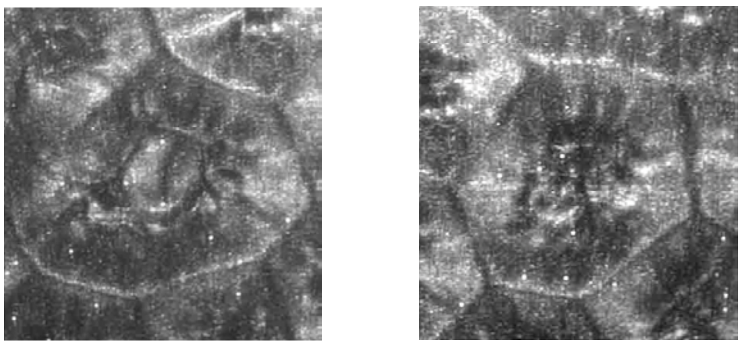

(a) (b)

Fig. 5. Photographs of (a) double cell structure and (b) spoke-like structure observed at $R_I^* \sim 20$.

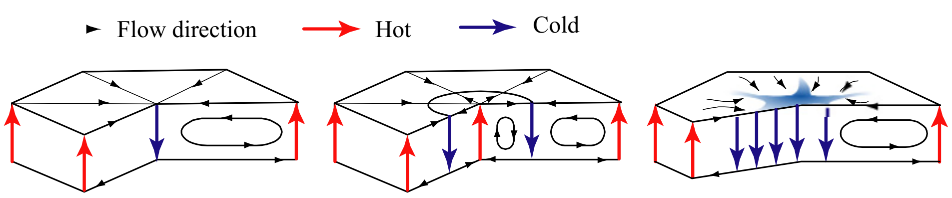


(a) (b) (c)

Fig. 6. Schematic illustrations of the cell structures; (a) regular hexagon, (b) double cell structure and (c) spoke-like structure.

# 4. Conclusion

In order to confirm the cell dilatation, an experiment that is more closely approximated by the theoretical models was performed. The thermal boundary condition at the bottom plate became nearly adiabatic by using vacuumed glass as the bottom plate, and the non-uniformity of the internal heating was reduced by increasing the height of the fluid layer. Fluid motion was visualized to estimate the cell dilatation using Kalliroscope. With the improvements of the experimental setup in the present study, cell dilatation could be observed in digital photographs for each $R_I^*$. We conclude, therefore, that the dilatation of a convection cell with respect to internal Rayleigh number is characteristic of natural convection induced by internal heat generation (we mentioned that the cell dilatation was also observed in Rayleigh-Benard convection (e.g., Koschmieder, 1993)), but the rate of the expansion is smaller than this phenomenon.). The cell dilatation may be related to the enhancement of "cold plume"; the cold plume, which is a separated thermal boundary layer from the top boundary, induces convective motion and sweeps high temperature fluid at the lower part of the fluid layer. This sweep is enhanced with respect to Rayleigh number.

As a result of the cell dilatation, an expanded cell breaks up and a smaller cell appears in the expanded cell like double structure as mentioned in Schwiderski and Schwab (1971) (double cell structure). When the hexagonal shape of the cell is relatively regular, the small cell is not formed and the descending flow region expands laterally like a spoke as mentioned in Ichikawa, et al. (2006) (spoke-like structure). Such structures do not appear in the transition process to turbulent flow in standard Rayleigh-Bénard convection, as shown in the phase diagram (Krishnamurti, 1970).

## *References*


Carrigan, C. R., Convection in an internally heated, high Prandtl number fluid: a laboratory study, Geophys. Astrophys. Fluid Dyn. 32 (1985), 1-21.

Ichikawa, H., et al., Cell pattern of thermal convection in induced by internal heating, Phys. Fluids, 18 (2006), 038101.

Koschmieder, E. L, Bénard Cells and Taylor Vortices, (1993), Cambridge University Press, Cambridge.

Krishnamurti, R., On the transition to turbulent convection. Part 2. The transition to time-dependent flow, J. Fluid Mech., 42 (1970), 309-320.

Roberts, P. H., Convection in horizontal layers with internal heat generation: theory, J. Fluid Mech., 30 (1967), 33-49.

Schubert, G., Turcotte, D. L. and Olson, P., Mantle convection in the earth and planets, (2001), Cambridge Univ. press, Cambridge.

Schwiderski, E. W. and Schwab, H. J., Convection experiments with electrolytically heated fluid layers, J. Fluid Mech., 48 (1971), 703-719.

Tasaka, Y., et al., Experimental investigation of natural convection induced by internal heat generation, J. Phys: Conference Series, 14 (2005), 168-179.

Tasaka, Y., Ito, K. and Iima, M., Visualization of a rotating flow under large-deformed free surface using anisotropic flakes, J. Visualization, 11-2 (2008), 163-172.

Thoroddsen, S. T. and Bauer, J. M., Qualitative flow visualization using colored lights and reflective flakes, Phys. Fluids, 11-7 (1999), 1702-1704.

Tritton, D. J., Internally heated convection in the atmosphere of Venus and in the laboratory, Nature, 257 (1975), 110.

Tritton, D. J. and Zarraga, N. M., Convection in horizontal layers with internal heat generation: experiments, J. Fluid Mech., 30 (1967), 21-32.

Turcotte, D. L., Schubert, J. and Schubert, G., Geodynamics 2nd edition, (2001), Cambridge Univ. press, Cambridge.


## *Author Profile*

Yuji Tasaka: He received his M. Sc. (Eng). in Mechanical Engineering in 2002 from Hokkaido University. He also received his Ph.D. in Mechanical Engineering in 2005 from the same university. He worked in the Graduate School of Engineering, Hokkaido University as a research associate. He is an assistant professor since 2006. His research interests are ultrasonic measurement of liquid metal flow, especially thermal convection, flow instability and transition processes from laminar flow to turbulent flow.

Kengo Yonekura: He received his M.Sc. (Eng.) degree in Mechanical Engineering in 2003 from Hokkaido University. After obtaining M. Sc. he works as an engineer at Nissan Motor Co., Ltd.

Yasushi Takeda: He received his M. Sc. (Eng) in Engineering School in 1970 from Tohoku University, and received his Ph.D. (Eng) in 1979 from the same university. He worked in Department of Engineering, Tohoku University as an instructor till 1981 and then moved to Swiss Institute for Nuclear Research. He worked in Paul Scherrer Institute Switzerland as a Senior Researcher since 1988 before he became a professor of Hokkaido University. During his long visit in PSI he received his second title of Ph. D. (Science) from The University of Tokyo in 1996. His research interests are ultrasonic velocity profiling (UVP), flow measurement methodology, vortex dynamics and transition to turbulence.

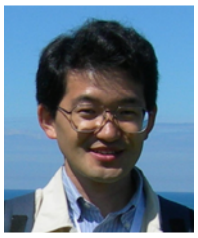

Takatoshi Yanagisawa: He received his M. Sc. in Graduate School of Science in 1995 from University of Tokyo, and received his D. Sc. in 1998 from the same university. He worked as JSPS post doctoral fellow in Graduate School of Science, University of Tokyo till 2001, and now he is working at Institute for Research on Earth Evolution (IFREE), Japan Agency for Marine-Earth Science and Technology (JAMSTEC). His research interests are the flows of Earth's deep interior, mantle convection and outer-core convection.